



OPEN ACCESS

EDITED BY

Lujun Shen,
Sun Yat-sen University Cancer Center
(SYSUCC), China

REVIEWED BY

Sandra Lettlova,
University of Zurich, Switzerland
Hao Cheng,
Fudan University, China

*CORRESPONDENCE

Jiong Lu
✉ lujiongmail@163.com
Bei Li
✉ libei@scu.edu.cn

[†]These authors have contributed
equally to this work

SPECIALTY SECTION

This article was submitted to
Gastrointestinal Cancers: Hepato
Pancreatic Biliary Cancers,
a section of the journal
Frontiers in Oncology

RECEIVED 12 November 2022

ACCEPTED 09 January 2023

PUBLISHED 09 February 2023

CITATION

Nie G, Peng D, Wen N, Wang Y, Lu J and
Li B (2023) Cuproptosis-related genes
score: A predictor for hepatocellular
carcinoma prognosis, immunotherapy
efficacy, and metabolic reprogramming.
Front. Oncol. 13:1096351.
doi: 10.3389/fonc.2023.1096351

COPYRIGHT

© 2023 Nie, Peng, Wen, Wang, Lu and Li.
This is an open-access article distributed
under the terms of the [Creative Commons
Attribution License \(CC BY\)](https://creativecommons.org/licenses/by/4.0/). The use,
distribution or reproduction in other
forums is permitted, provided the original
author(s) and the copyright owner(s) are
credited and that the original publication in
this journal is cited, in accordance with
accepted academic practice. No use,
distribution or reproduction is permitted
which does not comply with these terms.

Cuproptosis-related genes score: A predictor for hepatocellular carcinoma prognosis, immunotherapy efficacy, and metabolic reprogramming

Guilin Nie^{1†}, Dingzhong Peng^{2†}, Ningyuan Wen¹, Yaoqun Wang¹,
Jiong Lu^{1,3*} and Bei Li^{1,3*}

¹Department of Biliary Surgery, West China Hospital of Sichuan University, Chengdu, China,

²Department of General Surgery, Division of Hepatobiliopancreatic Surgery, Nanfang Hospital, Southern
Medical University, Guangzhou, Guangdong, China, ³Research Center for Biliary Diseases, West China
Hospital, Sichuan University, Chengdu, Sichuan, China

Background: Cuproptosis is a newly identified type of programmed cell death, characterized by aggregation of mitochondrial lipoylated proteins and the destabilization of Fe–S cluster proteins triggered by copper. However, its role in hepatocellular carcinoma (HCC) remains unclear.

Methods: We analyzed the expression and prognostic significance of cuproptosis-related genes using the data obtained from TCGA and ICGC datasets. A cuproptosis-related genes (CRG) score was constructed and validated *via* least absolute shrinkage and selection operator (LASSO) Cox regression, multivariate Cox regression and nomogram model. The metabolic features, immune profile and therapy guidance of CRG-classified HCC patients were processed *via* R packages. The role of kidney-type glutaminase (GLS) in cuproptosis and sorafenib treatment has been confirmed *via* GLS knockdown.

Results: The CRG score and its nomogram model performed well in predicting prognosis of HCC patients based on the TCGA cohort (training set), ICGC cohort and GEO cohort (validation set). The risk score was proved as an independent predictor for overall survival (OS) of HCC. The area under the curves (AUCs) of the model in the training and validation cohorts were all around 0.83 (TCGA, 1- year), 0.73 (TCGA, 3- year), 0.92 (ICGC, 1- year), 0.75 (ICGC, 3- year), 0.77 (GEO, 1- year), 0.76 (GEO, 3- year). Expression levels of metabolic genes and subtypes of immune cells, and sorafenib sensitiveness varied significantly between the high-CRG group and low-CRG group. One of the model-included gene, GLS, might be involved in the process of cuproptosis and sorafenib treatment in HCC cell line.

Conclusion: The five cuproptosis-related genes model contributed to prognostic prediction and provided a new sight for cuproptosis-related therapy in HCC.

KEYWORDS

cuproptosis, hepatocellular carcinoma, prognostic model, sorafenib, GLS

Introduction

Several types of regulated programmed cell death have been reported, including apoptosis, pyroptosis, necroptosis, and ferroptosis (1). Ferroptosis, a unique modality of cell death driven by iron-dependent phospholipid peroxidation, is regulated by complex cellular metabolic events, including redox homeostasis, iron handling, mitochondrial activity, and amino acids metabolism, lipid metabolism, sugar metabolism, in addition to numerous signaling pathways relevant to disease (2–4). Similar to iron, copper is a cofactor for essential enzymes and has been recognized to induce the aggregation of lipoylated dihydrolipoamide S-acetyltransferase (DLAT) caused by FDX1. Lipoylated DLAT is associated with the mitochondrial tricarboxylic acid (TCA) cycle, resulting in proteotoxic stress and a novel form of cell death called “cuproptosis” (5). In brief, the copper-induced death was independent of known cell death pathway and relied on mitochondrial metabolism. The new mechanistic information suggests that other trace metalion-induced forms of cell deaths exist (6). Similar to ferroptosis induction-based cancer therapies in nanoparticle-based gene-target therapies or in combination with other therapeutic approaches (7), cuproptosis induction-based treatment provides new therapeutic approaches for cancers with the development of cuproptosis-related research.

The role of copper in the development of HCC remains unknown. Otherwise, some studies have proved that copper contributes to hepatocarcinogenesis and its progression. Copper contributes to glycolytic metabolism and the tumorigenic properties of hepatocellular carcinoma (HCC) (8). A copper complex, $[\text{Cu}(\text{tpp}-\text{tpp})\text{Br}^2]\text{Br}$ (referred to as CTB), could induce HCC cells senescence and act as an antitumor compound *via* SLC25A26 and methionine cycle (9). Disulfiram combined with copper inhibits metastasis and epithelial-mesenchymal transition in HCC *via* NF- κ B and TGF- β pathways (10). The copper metabolism MURR1 domain 10 (COMMD10) increased intracellular Cu and led to radioresistance of HCC (11). In addition, the increased incidence of HCC in patients and animal models with Wilson disease was found to be associated with an unknown mechanism promoting the malignant process resulting from copper accumulation (12). The emergence of cuproptosis provides new insights into copper-based therapies for HCC.

This study explored the mechanism of copper-induced cell death underlying HCC. We rescreened the genes involved in copper ionophore-induced death. The data was acquired from the genome-wide CRISPR-Cas9 loss-of-function screens dataset provided by Peter Tsvetkov (5). The association between cuproptosis-related genes and HCC prognosis was explored and the genes were used to establish a prognosis-predicted model, which demonstrated potential in grading HCC in terms of copper-induced cell death.

Materials and methods

Public data acquisition and processing

The cuproptosis-related genes datasets were acquired from the Tsvetkov’s study. The gene expression data, phenotype data, and corresponding survival information (if available) of HCC of The Cancer Genome Atlas (TCGA), the liver cancer project (code: LIRI_JP) of the International Cancer Genome Consortium (ICGC), and GSE14520 were

downloaded from public databases. The single-cell analysis of GLS, FDX1, and CDKN2A in HCC was conducted in the Tumor Immune Single-Cell Hub (TISCH) database (<http://tisch.comp-genomics.org/>) and used the data from GSE125449. Additional ethical approval was not required since these data were all publicly available online.

Construction and validation of a cuproptosis-related gene model

OVISe cells were used to screen cuproptosis-related genes. The OVISe-Cas9 cells were then infected with Brunello virus obtained from the Brunello virus library, which contains 76411 sgRNAs targeting 19114 genes. After the primary treatment of 50nM elesclomol-Cu, 200nM Cupric diethyldithiocarbamate (Cu-DDC), or DMSO control to the final dose of 250nM elesclomol-Cu and 700nM Cu-DDC, genomic DNA was isolated and sequenced by the Broad Genetic Perturbation Platform and Broad Genomics Platform for the establishment of gene library (5). The different expression genes were computed and considered as cuproptosis-related genes with an FDR < 0.05. 27 genes were possibly involved in copper ionophore-induced cell death and 25 genes expression levels (AFG3L2, AHR, BRPF1, CAPRIN1, CDKN2A, COQ7, DLAT, DLD, EGLN1, FDX1, GLS, HAUS5, LIAS, LIPT1, MBTPS1, MTF1, OXA1L, PDHA1, PDHB, REXO2, RPL3, SCAP, SLFN11, SOX2, YEATS20) except MCUR1 and MPC1 were detected in the TCGA dataset and put into the LASSO regression *via* the algorithm. We utilized the “glmnet” package (version 2.0-16) to fit the logistic LASSO regression. The optimal penalty coefficient ($\lambda = 0.00542$) in the LASSO regression was identified with the minimum criterion and five genes (FDX1, GLS, CDKN2A, DLAT, and LIAS) were found out as independent risk factors for HCC patients. Ten-fold cross-validation was used to select the penalty term, λ . The binomial deviance was computed for the test data as the measure of the predictive performance of the fitted models. The standard errors of the LASSO coefficients were obtained *via* bootstrapping within the primary sampling unit and strata (13). To performed the HRs of related genes, we showed totally ten HRs of genes included in the LASSO regression.

Gene signature model construction and validation of predictive nomogram

Nomograms are widely used to predict the survival probability of cancer. Clinical characteristic parameters and prognostic signature were adopted to establish a nomogram to quantitatively investigate the probability of 1-, 3-, and 5-year survival of HCC patients. To construct the nomogram, multivariate regression analysis was applied to select the significant predictors of mortality. The nomogram was trained using the TCGA data and externally validated using the ICGC data. Discriminative performance was measured by concordance index (C-index). Calibration plots were used to describe the degree of fit between actual and nomogram-predicted mortality (14).

Enrichment analysis

Gene ontology (GO) annotation and Kyoto Encyclopedia of Genes and Genomes (KEGG) pathway enrichment analyses

between the two groups of patients were performed with the 'clusterProfiler' R package. An FDR <0.05 and $|\log_2FC| \geq 1$ was set as the cut-off values.

Immune profile analysis

The immune score and stromal score of each sample in the TCGA-LIHC cohort were calculated by the "estimate" package in R. The proportion of immune cells in the tumor microenvironment (TME) of each sample was evaluated *via* the TIMER, CIBERSORT, and CIBERSORT-ABS algorithm in R software. The single-sample gene set enrichment analysis (ssGSEA) with R package GSVA was used to evaluate the degree of 16 immune cells infiltration and the activity level of 20 immune-related functions in HCC samples. The differential expression of immune checkpoints between risk groups was analyzed *via* R package limma.

In vitro cell culture, maintenance, and transfection

The human HCC cell lines, PLC/PRF/5, and Huh7 were a gift from Professor Peng Yong (State Key Laboratory of Biotherapy, Sichuan University). Both cell lines were incubated at 37°C with 5% CO₂ in Dulbecco's Modified Eagle's Media (DMEM) (Gibco BRL, Grand Island, NY, USA) containing 10% FBS (Gibco, Australia). The cells were transfected with si-RNAs using Lipofectamine™ 3000 (Thermo Fisher Scientific, USA) in accordance with the manufacturer's instructions.

RNA preparation, reverse transcription, and quantitative real-time PCR analysis

Total RNA was extracted using TRIzol Reagent (Invitrogen, Carlsbad, USA), and the concentration and purity of total RNA were determined by Nanodrop 2000 spectrophotometry (Thermo Scientific, USA). Reverse transcriptions were performed using Superscript III transcriptase (Invitrogen, Grand Island, NY). The cDNA amplification was performed using SYBR Green Real-time PCR Master Mix (Roche, Mannheim, Germany). 18S was used as the internal reference gene. The results were analyzed by the $2^{-\Delta\Delta Ct}$ method. The primer and si-RNA sequences were as follows: 5'-TTCCAGAAGGCACAGACATGGTTG-3' (forward) and 5'-GCCAGTGTGCGAGCCATCAC-3' (reverse) for GLS, and si-GLS: 5'-GAUGGACAGAGGCAUUCUA-3' (sense).

Western blot analysis

Protein was extracted from HCC cells using RIPA lysis buffer and quantified using a BCA kit (Thermo, USA). The protein samples were separated by 10% SDS-PAGE and transferred to PVDF membranes (Millipore, USA). After blocking for 1 h in 5% skim milk powder at room temperature, the membranes were incubated with primary

antibodies at 4°C overnight, followed by an incubation with an anti-rabbit secondary antibody (1:10000, Abcam, UK) and visualized using Immobilon™ Western Chemiluminescent HRP Substrate (Millipore, USA).

CCK8 assay

The effects of drugs and Copper on HCC cell lines were measured using CCK8 assay. Cells were seeded in 96-well plates at a density of 5×10^3 cells/well, cultured overnight, and subsequently treated with various concentrations of drugs or DMSO. A medium containing CCK8 reagent was added after exposing the cells to drugs, and the optical density (OD) value at 450 nm of each well was measured. Sorafenib was purchased from Selleck Chemicals (USA). Elesclomol was obtained from MCE (USA), CuCl₂ was from RHAWN (China).

Immunohistochemistry analysis

The protein expression levels of the selected genes in normal and tumor tissues were confirmed by the Human Protein Atlas database (HPA; <https://www.proteinatlas.org/>). The relative expression levels of GLS were measured *via* Image J (<http://rsb.info.nih.gov>).

Statistical analysis

R software (version 4.2.1) with the "ggplot2," "ggforest," "cowplot," "plot3D," "maftools," "VennDiagram," "survminer," "timeROC," and "ggplotify" packages, and GraphPad Prism (version 9.0) were used for statistical analysis and data visualization. For comparison between the two groups in the bioinformatics analysis section, the Wilcoxon test was used for difference analysis to compare the risk scores of the two groups. The Students'-test was used to compare between the two groups in the experimental section like PCR or IHC. Two-way ANOVA was used for the results of CCK. As for more than two groups, the Kruskal-Wallis test was used, like comparing the risk scores of the different pathological stages. Kaplan-Meier survival analysis and log-rank tests were used the survival analysis of the different groups of patients. The univariate and multivariate Cox regression with calculation of hazard ratios (HR) and 95% confidence intervals (CI) was used to evaluate the importance of each parameter to OS. The t-ROC analysis measured the predictive power of the risk model and the predictive power was showed as the area under the curve (AUC). A two-tailed $p < 0.05$ was considered statistically significant.

Results

FDX1, GLS, CKKN2A, DLAT, and LIAS were independent prognostic factors for HCC patients

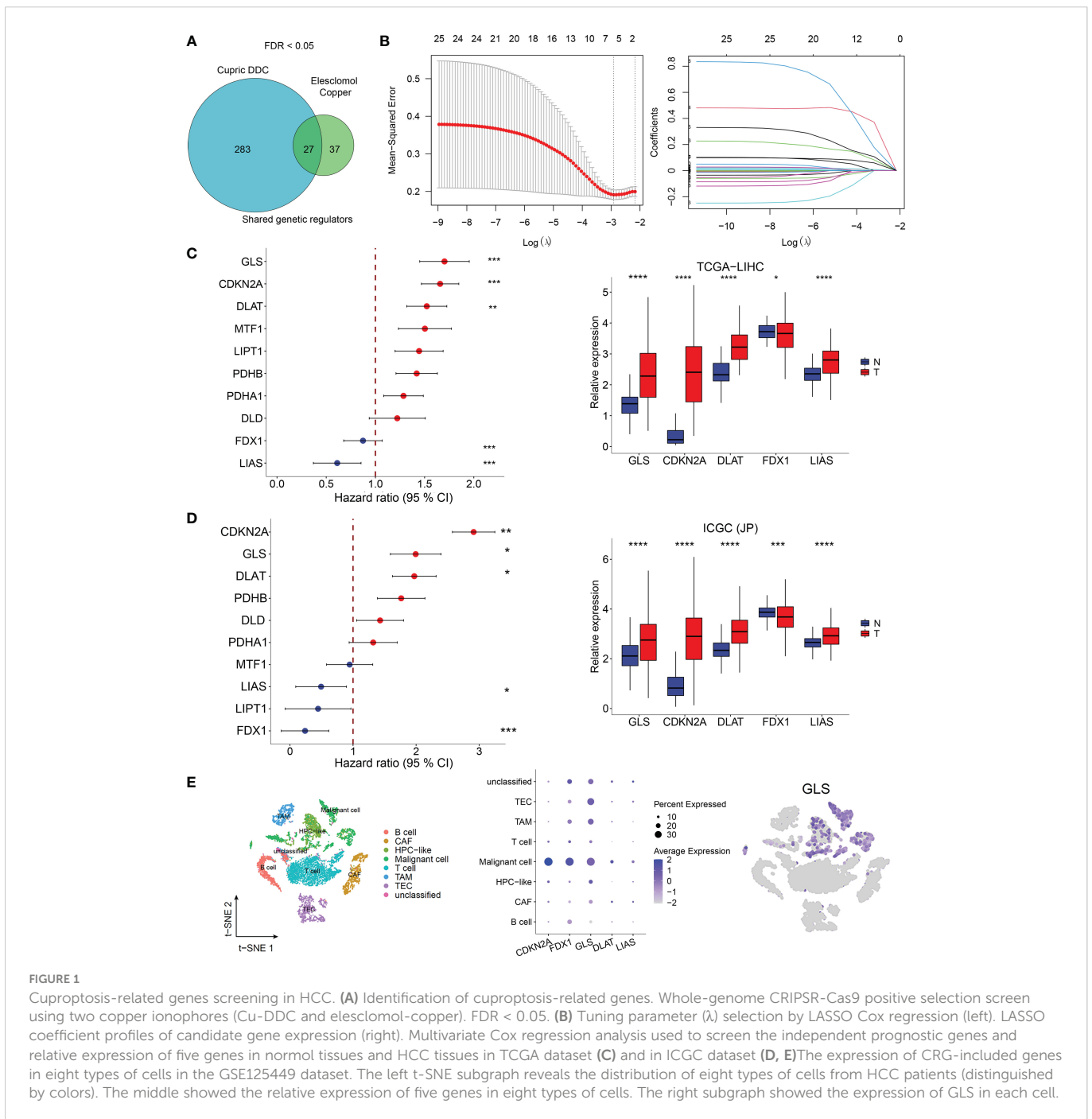
From the whole-genome CRISPR-Cas9 positive selection screen using two copper ionophores (Cu-DDC and elesclomol-copper) (FDR < 0.05),

we identified 27 genes possibly involved in copper ionophore-induced cell death (Figure 1A) and 25 genes were included in a LASSO regression model. The range of positive and negative standard deviations of $\log(\lambda)$ was identified in the cross-validation plot. A vertical line was drawn at the value selected *via* cross-validation analysis of 10-fold. The function of the analysis to select important variables develops with the increased degree of compression and decreased value of λ (13). The optimal penalty coefficient ($\lambda = 0.00542$) in the LASSO regression was identified with the minimum criterion (Figure 1B). The results of survival analysis obtained from TCGA and ICGC datasets showed that FDX1, GLS, CDKN2A, DLAT, and LIAS were independent factors for HCC patients and might contribute to predicting the prognosis of HCC. Meanwhile, they were differentially expressed in HCC tumor and normal tissues (Figures 1C, D). In addition,

single-cell sequence indicated that all five genes were included in GSE125449 and were predominantly detected in malignant cells (Figures 1E, S1).

High cuproptosis-related genes risk score predicted the poor outcome of HCC patients

A prediction model was constructed based on the patients' data from TCGA using a LASSO regression model and including the above five genes. The cuproptosis-related genes (CRG) risk scores = $0.53 \times \text{GLS} + 0.42 \times \text{DLAT} + 0.505 \times \text{CDKN2A} - 0.135 \times \text{FDX1} - 0.491 \times \text{LIAS}$.



The divided point of high risk and low risk was 4.6 (Figure 2A). The risk score distribution and outcome status showed that more deaths of HCC patients happened in higher risk score groups in our two cohorts (Figure 2B). The high-risk group had a shorter survival time than the low-risk group in the TCGA-LIHC dataset (training cohort, $p = 0.033$). Similar results were observed in the other two validation cohorts ($p = 8.4 \times 10^{-06}$ in ICGC-JP, $p = 0.036$ in GSE14520) (Figure 2C). The area under the curve (AUC) of the overall survival (OS) prediction model was 0.83 at one year and 0.73 at three years from TCGA. In the two external validation cohorts, the AUC values of the model in the ICGC-LIRI(JP) dataset were 0.92 at one year and 0.75 at three years, while they were 0.77 at one year and 0.76 at three years in the GSE14520 dataset (Figure 2D).

Development and validation of a comprehensive nomogram based on clinicopathological characteristics and CRG risk score for clinic application

We analyzed the relationship between the model and clinicopathological features of HCC patients. As shown in Figure 3A, age, gender, race, prior malignancy, and radiation therapy were not statistically meaningful for the prediction of prognosis. Otherwise, CRG scores were related to pathologic stage in the TCGA cohort and ICGC cohort (Figures S2A, B). On the other hand, the high score of the CRG model was an independent risk factor of low OS according to the clinical dates from TCGA ($HR = 1.5267$,

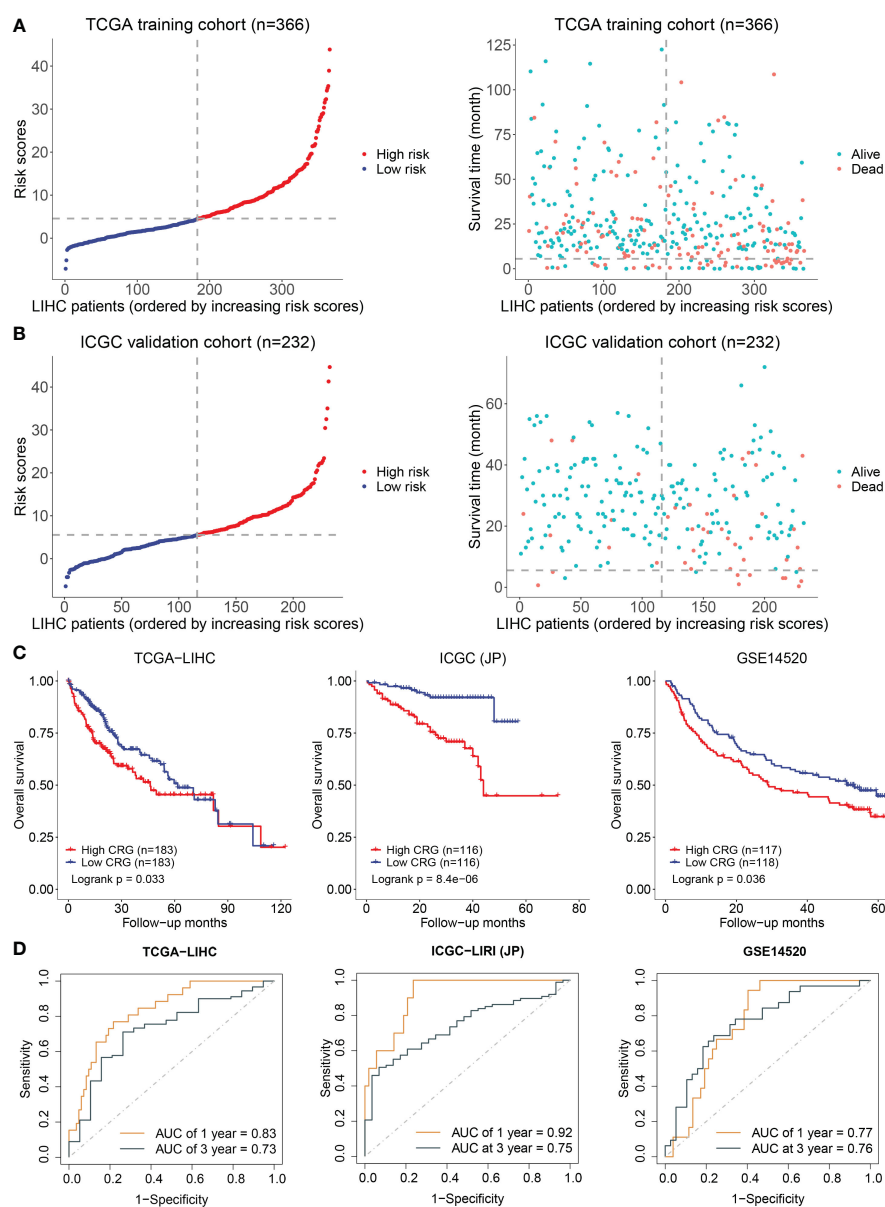


FIGURE 2

Establishment and validation of prediction model. (A) The distribution and optimal cutoff value of CRG (left), the OS status of each sample (right) according to TCGA dataset. (B) The CRG risk score status (left) and the OS status of each sample (right) according to ICGC dataset. (C) The Kaplan–Meier plots of CRG scores in the TCGA, ICGC, and GSE14520 cohorts based on the optimal cutoff value. (D) Time-dependent ROC analyses of the CRG for OS prediction in the TCGA, ICGC, and GSE14520 cohorts.

95%CI = 1.0144-2.298, $p = 0.04253$) (Figure 3A) and ICGC-LIRI(JP) (HR = 3.2132, 95%CI = 1.5607-6.6155, $p = 0.00153$) (Figure 3B). A nomogram was created to better quantify the predicted value of the risk model for individual HCC patients (Figures 3C, D), and the calibration curves showed the stability and accuracy of the risk model in the training and test cohorts (Figures 3E, F). The C-index was 0.66 in the TCGA group and 0.76 in ICGC-LIRI(JP) group.

The gene signature was closely related to a variety of metabolic characteristics of HCC

Cuproptosis is characterized by the aggregation of lipoylated proteins, which were involved in the process of the TCA cycle occurring in the mitochondria (6). The link between cuproptosis and mitochondrial proteins indicated that the effect of CRG risk score on

metabolism in HCC needs to be further clarified. Gene set enrichment analysis (GSEA) based on the TCGA dataset for the two groups showed that HCC patients in the low-CRG group had enrichments in metabolism-related pathways such as pyruvate metabolism, fatty acid metabolism, alanine-aspartate-glutamate metabolism or glutathione metabolism (Figure 4). Specifically, Glutamine is considered as the second important nutrient only to glucose in cancer. Its metabolism begins with the conversion to glutamate by GLS (15). The glutamate could be transferred into mitochondria, transformed to alpha-ketoglutarate and participated in the TCA cycle. As for glutathione (GSH), despite being produced exclusively in the cytosol with the utilization of cysteine, glutamate or glycine, GSH is also abundant in many organelles, including peroxisomes, the nucleus, endoplasmic reticulum and mitochondria (16). The enrichment analysis confirmed that the metabolism-related changes of high-CRG HCC patients centralized in pyrimidine metabolism or purine metabolism. The

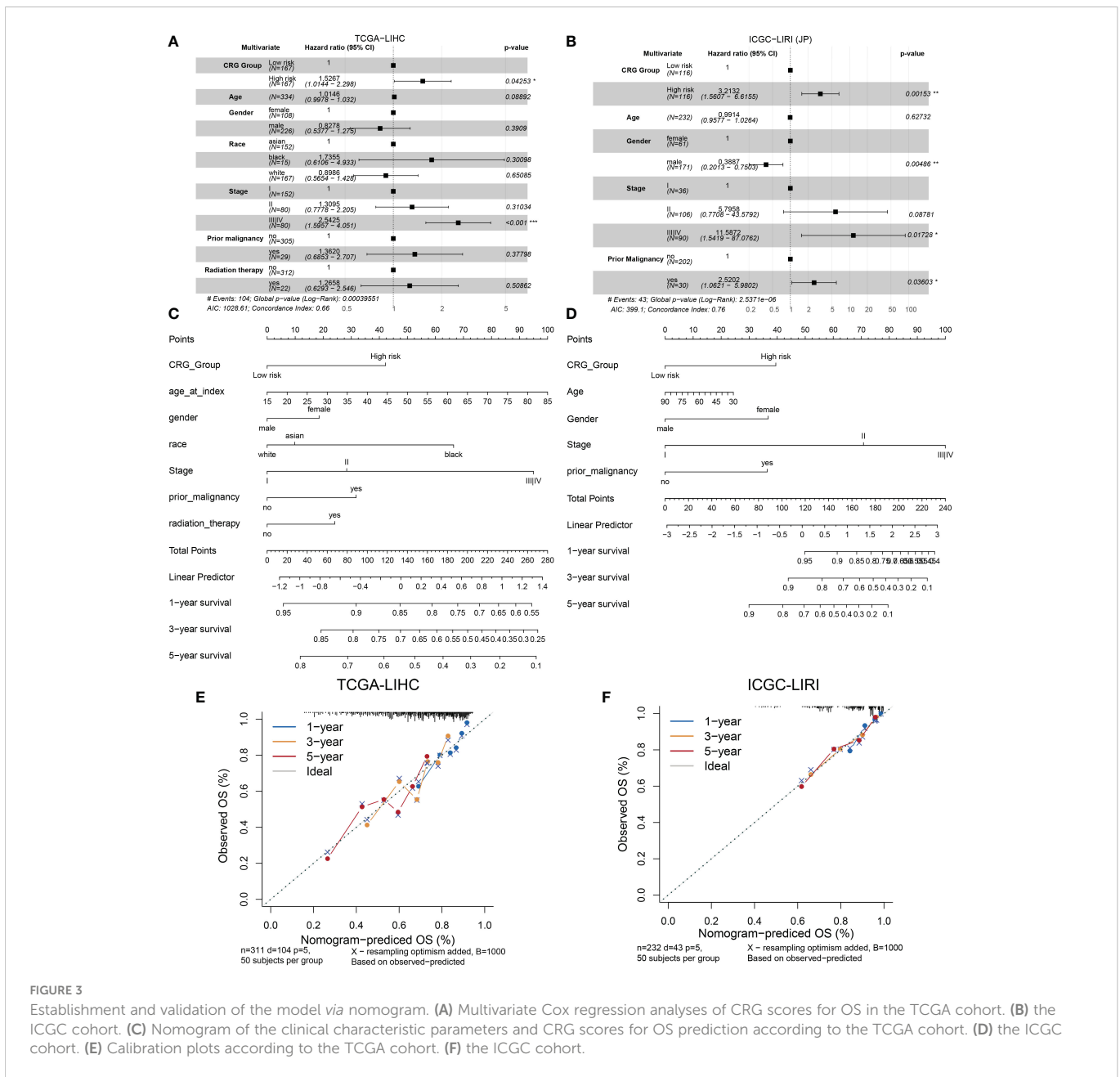


FIGURE 3 Establishment and validation of the model via nomogram. (A) Multivariate Cox regression analyses of CRG scores for OS in the TCGA cohort. (B) the ICGC cohort. (C) Nomogram of the clinical characteristic parameters and CRG scores for OS prediction according to the TCGA cohort. (D) the ICGC cohort. (E) Calibration plots according to the TCGA cohort. (F) the ICGC cohort.

pyrimidine metabolism together with purine metabolism, final generates deoxyribonucleoside triphosphates (dNTPs) in the nucleus, cytoplasm and mitochondria for cell proliferation (17) (Figure 4). In our article, we only initially analyzed the varied performance of metabolism-related pathways in two groups. Metabolomics analysis of clinic samples could be used to judge the changes in metabolic substrate and for deeper exploration.

The gene signature served as a valuable marker for immune targets and immunotherapy response

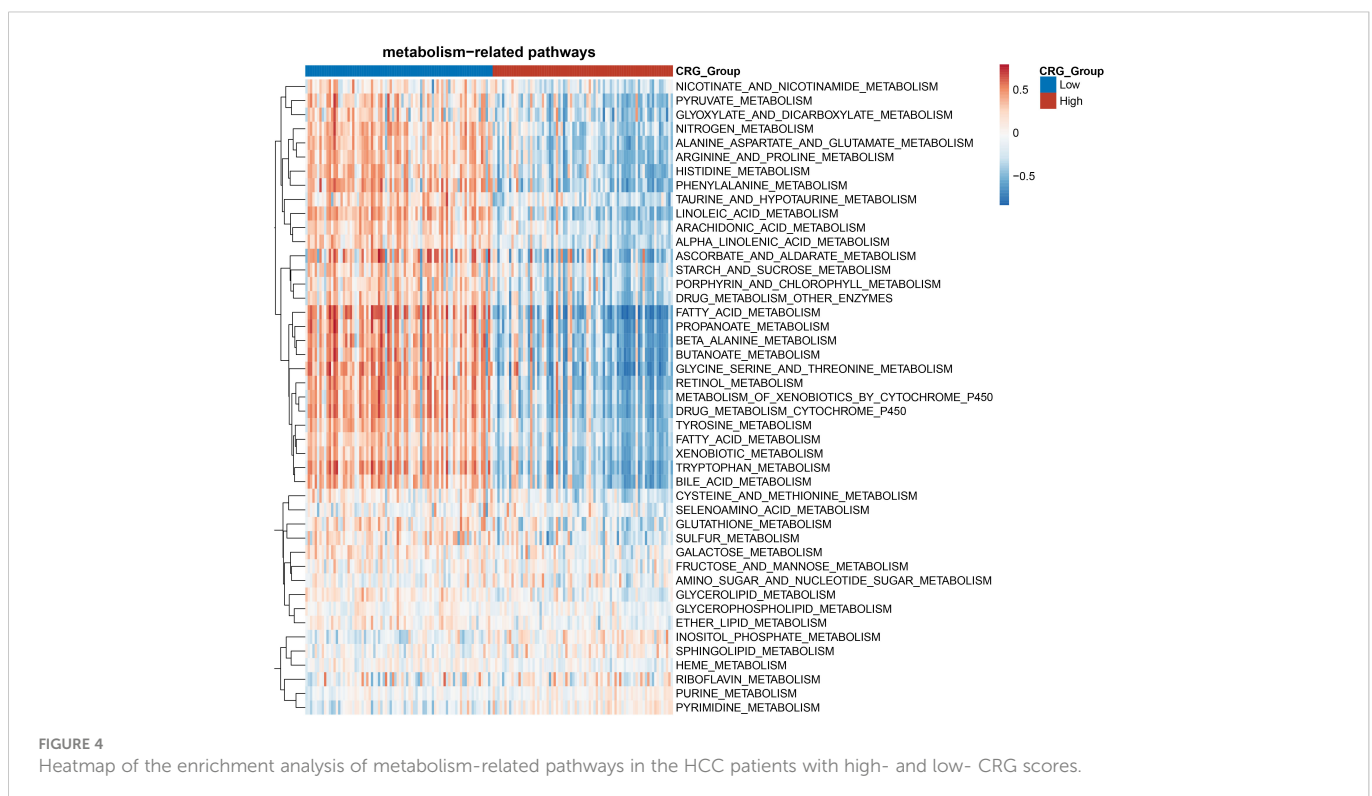
Tumor immunology plays a key role in HCC development and progression (18). We evaluated the immune landscape of CRG and found that high-CRG patients had significantly higher immune scores than low-CRG patients. Besides, using the TIMER algorithm, we initially noticed different scores of macrophages, B cells, CD4+ T cells, and neutrophils in two groups (Figure 5A). According to the results of the CIBERSORT and CIBERSORT-ABS algorithm, more specific features were presented in subtypes of immune cells, such as macrophage M0, M1, and M2 (Figure 5B). Immune infiltration scores of macrophages M0 were higher in the high-risk group in the CIBERSORT, while the other two subtypes showed no statistically significant difference between the two groups. Based on CIBERSORT-ABS, all three subtypes in the high-risk group were higher than the low-risk group ($p < 0.01$) (Figures S3A, B). We performed an ssGSEA analysis to observe immune cell subpopulations, immune functions, and pathways in the high-risk and low-risk groups or risk scores. The results showed that the immune cells including macrophages myeloid DC, Tregs cell, neutrophil and CD4+ Th2 cell were markedly

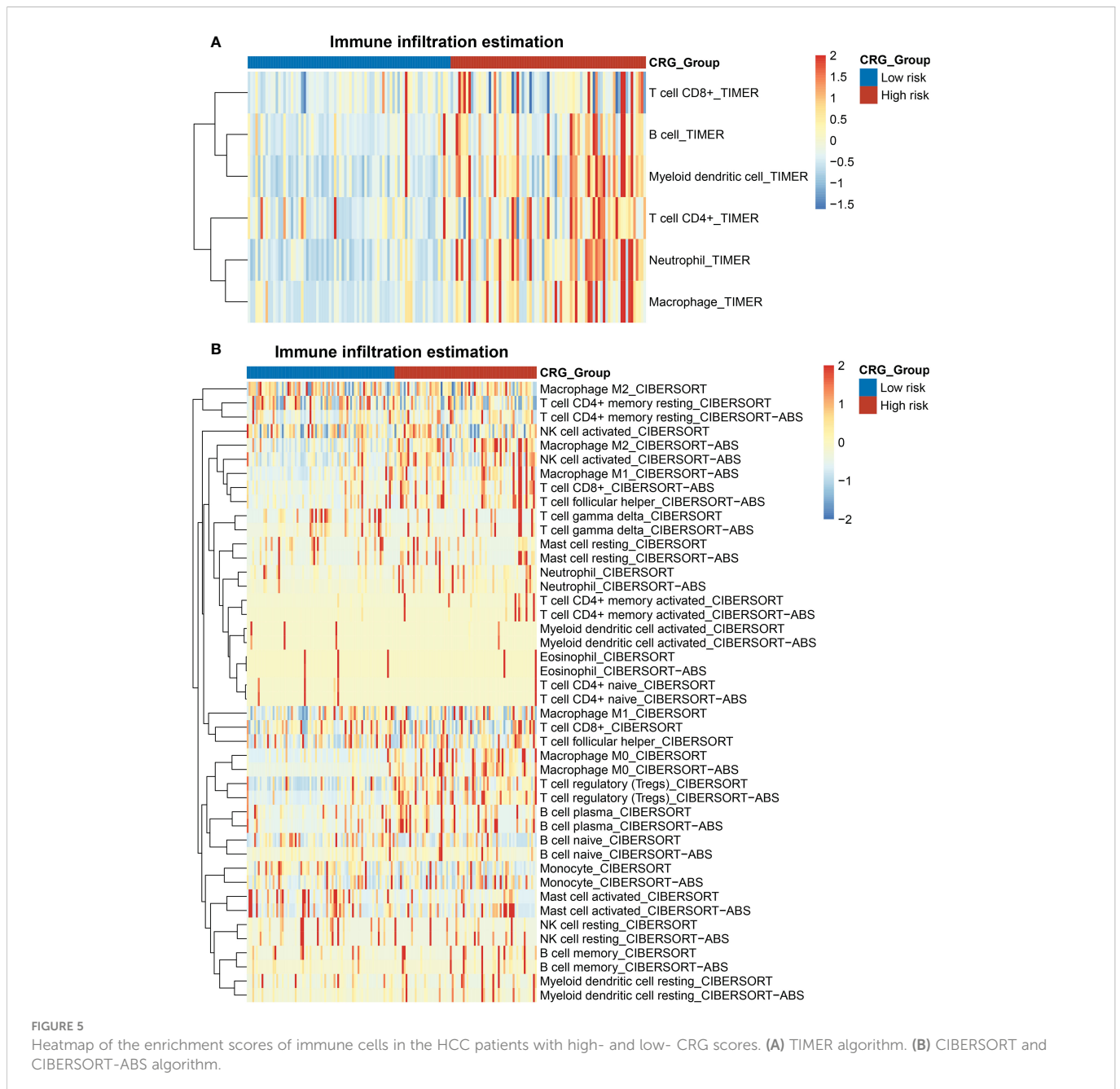
expressed in the high-risk group of the TCGA cohort ($p < 0.05$) (Figure S4). Regarding immune function, the risk levels of lipid mediators, glycogen metabolism, glucose deprivation and TCA cycle were higher in the low-risk group than in the high-risk group, when the functionality of the G1/S and G2/M was opposite to these functions (Figure S5). Immune checkpoints in high- and low-CRG groups relying on TCGA dataset were found to be different, such as BN2A1, BTN2A2, CD276, CD47, CD70, and HLA all highly expressed in high-CRG groups (Figure S6A). As for PD-L1, the expression of PD-L1 of high-CRG group was higher in both datasets (Figures S6B, C), which proved the correlation between PD-L1 and cuproptosis.

Sorafenib worked as the first-line treatment for advanced-stage HCC patients (19). Therefore, we evaluated the effect of sorafenib for different CRG risk patients and found that the response of sorafenib treatment followed the relative expression of GLS, DLAT, FDX1, and LIAS and risk scores of CRG (Figures 6A, B) (GSE109211). Patients with a lower score were more sensitive to sorafenib treatment ($p < 0.01$). Similar results were observed in the analysis for transcatheter arterial chemoembolization (TACE) treatment, a widely used therapy for HCC patients at stage BCLC A or B (20). Patients who responded to TACE treatment had significantly variations in expression levels of GLS, CDKN2A, FDX1 and higher values of CRG ($p = 0.0011$) (Figures 6C, D).

GLS was associated with poor prognosis and cuproptosis in HCC

GLS had the highest HR in the multivariate Cox regression analysis and dropped our attention. The expression level of GLS was





related to pathologic stage in the TCGA cohort (Figure S7A). We initially validated the function of CuCl_2 in the HCC cell line (PLC and Huh7) related to cuproptosis *via* elesclomol. The results confirmed that the addition of Cu^{2+} enhanced the effect of elesclomol (Figure 7A). The decreased expression of the GLS gene reduced the cell death induced by elesclomol-Cu (Figures 7B, S7B, C). In addition, when the GLS gene was knocked down in PLC and Huh7, they were more sensitive to sorafenib (Figure 7C), corresponding to the previous prediction. The immunohistochemical staining for GLS highlighted its high expression in HCC tissue (Figure 7D). Percentage of positive of HCC group including low positive, positive, high positive, is about 61%. Percentage of positive of non-HCC group is about 24%. After systemically analyzing three databases (Figure 7E), GO analysis showed that they were enriched in actin binding, Ras GTPase binding and so on (Figure 7F). Meanwhile,

KEGG analysis indicated that GLS was related to Ras signaling pathway (Figure 7G). In summary, *in vitro*, experimental data suggest that high expression of GLS is related to cuproptosis and poor prognosis in patients with HCC.

Discussion

Traditionally, copper was recognized as an active site cofactor to mediate a variety of essential cellular functions, such as antioxidant defense, biosynthesis of hormones, pigments, neurotransmitters and mitochondrial respiration (21–23). This has been challenged by its newly-discovered role of dynamic signaling metal and metalloallosteric regulator that promote copper-dependent cell proliferation (cuproplasia) and copper-dependent cell death

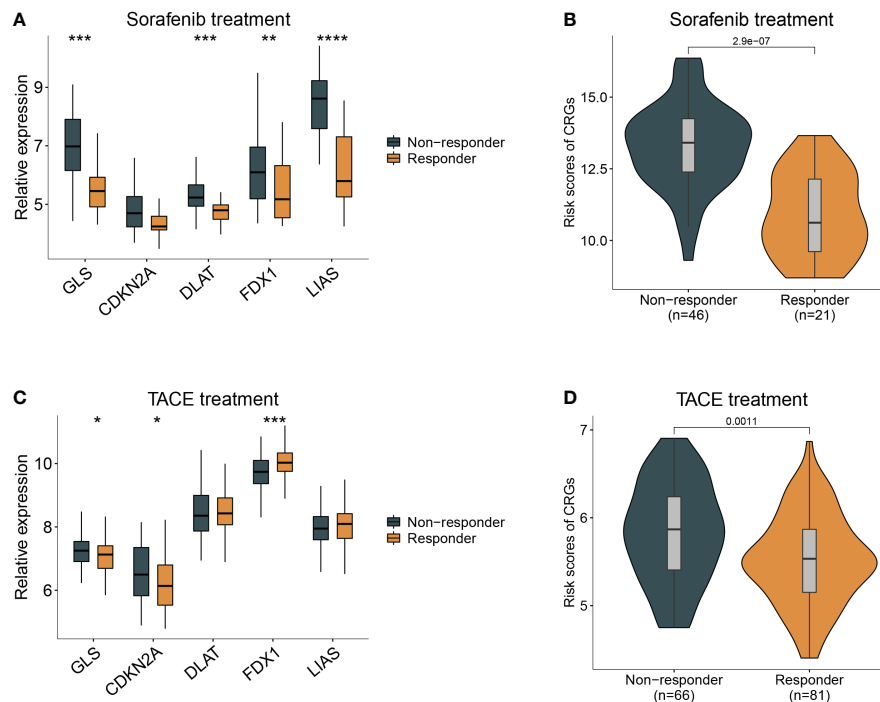


FIGURE 6

Guidance of CRG score in the therapy for HCC patients. (A) The different responses to sorafenib in the HCC patients with different expression of cuproptosis-related genes. (B), with high- and low- CRG scores. (C) The different responses to TACE treatment in the HCC patients with different expression of cuproptosis-related genes. (D), with high- and low- CRG scores. Wilcoxon test was used for data analyses.

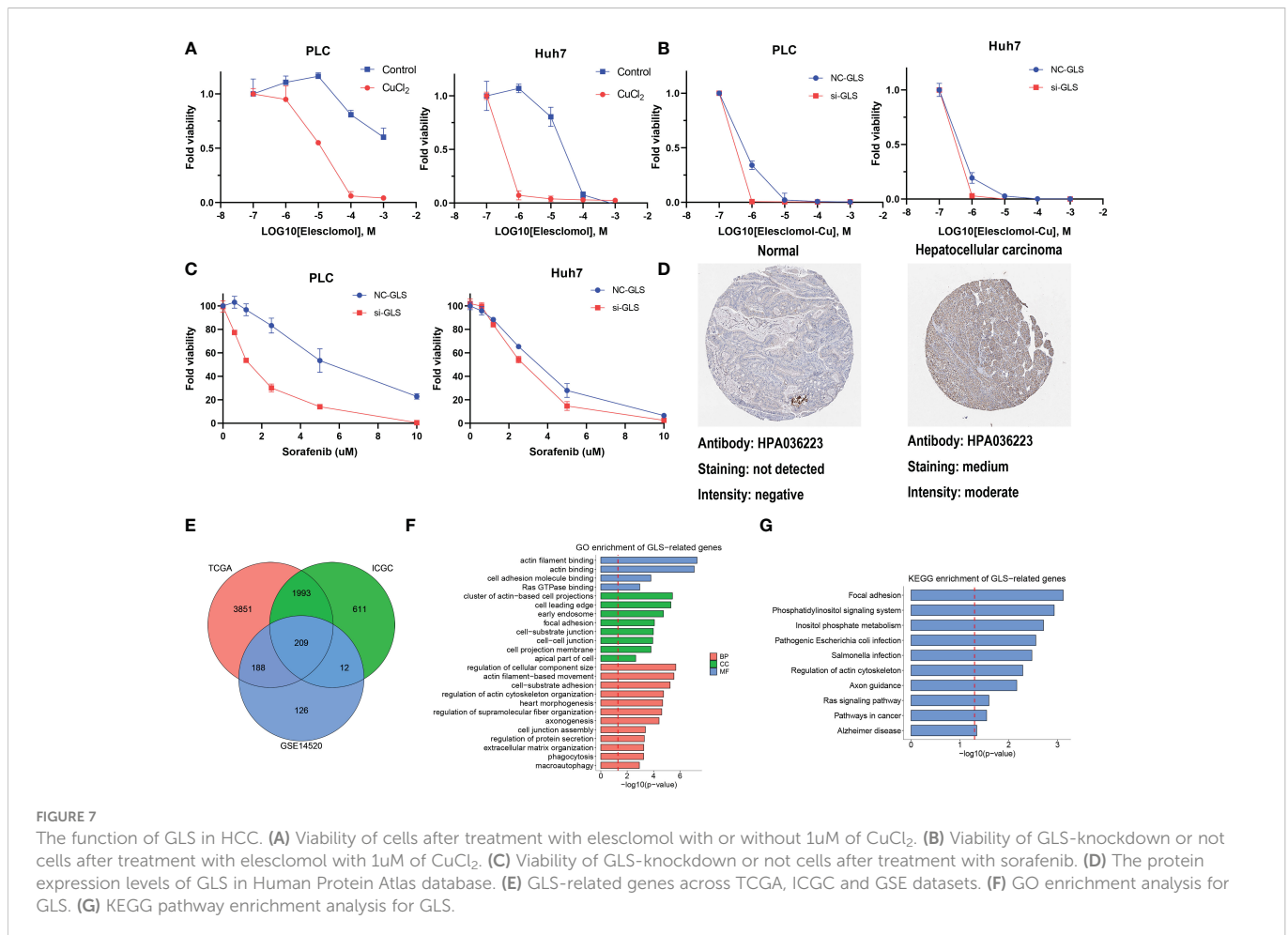
(cuproptosis) (24). According to recent studies, cuproptosis was characterized by the aggregation of mitochondrial lipoylated proteins and the destabilization of Fe-S cluster proteins triggered by copper (6). The liver is a major site of copper storage and removal. Some studies have demonstrated the role of copper in tumorigenesis and the development of HCC (25, 26). The increased incidence of HCC in patients with Wilson disease highlights the unknown mechanism of copper-related malignant transformation (27). In addition, previous studies have established the correlation between serum copper level and overall survival or other prognostic indicators (28, 29). Although decades of studies highlight the interplay between copper and HCC, a systemic molecular explanation of copper does not perform from present researches, and few studies have provided insights into the role of cuproptosis in HCC progression.

Here, we obtained 27 cuproptosis-related genes from a previous study with a FDR score <0.05 . The LASSO regression detected that only five (FDX1, GLS, CDKN2A, DLAT, and LIAS) possessed compatible prognostic values considering their expression level and molecular function. The differential expression gene analysis of the TCGA dataset identified all five candidate genes, and FDX1, encoding a small iron-sulfur protein, was recently found to regulate dihydrolipoamide S-acetyltransferase (DLAT) lipoylation and facilitates the oligomerization of lipoylated DLAT (5). The above process attributed to copper-related cell death in a completely different way from apoptosis, pyroptosis, necroptosis, or ferroptosis. GLS encodes a K-type mitochondrial glutaminase, which mainly participates in glutamine metabolism and glutathione (GSH) production (30). GLS could regulate stemness properties of cancer stem cells by increasing ROS accumulation and suppressing the Wnt/

β -catenin pathway in HCC (31). CDKN2A (cyclin-dependent kinase inhibitor 2A) is related to three alternatively spliced variants: two kinds of CDK4 kinase or a stabilizer of the tumor suppressor protein p53 (32). CDKN2A was reported to be a tumor suppressor gene. However, it is a highly-expressed gene associated with poor prognosis and immune infiltration in HCC patients (33). As a member of the radical S-adenosylmethionine (SAM), human lipoyl synthase (LIAS) is an enzyme containing two [4Fe-4S] clusters involved in the biosynthesis of the lipoyl cofactor (34). By lipoylation of E2 subunit (dihydrolipoyl succinyltransferase [DLST]) within the mitochondria, LIAS was involved in tricarboxylic acid (TCA) cycle process (35). In addition, the results of the single-cell sequence confirmed that FDX1, GLS, and CDKN2A were predominantly detected in malignant HCC cells, suggesting the involvement of cuproptosis-related genes in the development of HCC.

In the risk genes model, the high-CRG group showed a considerably shorter survival time, and the model performed satisfactorily for prognostic prediction in the training and validation cohorts. The external validation of our model in clinical settings revealed that the prognostic risk score model was an independent prognostic indicator. In addition, a risk-assessment nomogram was used to evaluate the potential clinical application of this model.

We focused on the metabolic and immunological pathways to establish a biological landscape of two groups divided by our five-genes model. The immunologic and metabolic pathways play a leading role in tumorigenesis of HCC, and was chosen as targets of therapeutic researches. Cuproptosis relied on the mitochondrial TCA cycle and was influenced by oxygen concentration (5). The metabolism-related pathways analysis corroborated with previous results. The low-risk group showed



enrichments in mitochondrial metabolism and aerobic glycolysis, such as pyruvate and glutathione metabolism. Otherwise, the low-risk group involved the enrichment of fatty acid metabolism, bile acid metabolism, and amino acid metabolism like alanine, arginine, serine, and glycine, which might be related to oxidative stress. The results of immune infiltration estimation showed the macrophage scores varied in the two groups. The resting macrophages (M0) could be polarized into different phenotypes, pro-inflammatory (M1) or anti-inflammatory (M2) (36). M1 were reported to potentially participate in antitumor immunity. Conversely, M2 could enhance tumor progression by promoting angiogenesis, fibrosis, immunosuppression, lymphocyte exclusion, invasion, and metastasis (37). Nevertheless, how cuproptosis or cuproptosis-inducing drugs affect the function of antitumor immune cells and the metabolic changes remains unclear.

GLS was known as a mitochondrial glutaminase, increasing glutathione and glutamine levels. In a recent study, treatment of HCC cell lines (HCCLM3, SMMC-7721, and Hep3B) with GLS1 inhibitors halted the growth of HCC cell lines (38). As shown in the “Cuproptosis” article, GSH inhibited cuproptosis *via* copper(I), where Chung et al. established the relevance of copper and glutathione in cancer cells. Their work revealed that oncogene-driven changes in the metabolism of glutathione lead to a labile copper(I) deficiency, insinuating that lower GSH/GSSG ratios decreased labile copper(I) availability but did not affect total copper level (39). The theory suggests that copper(I) ion, which is essential for DLAT aggregation and cuproptosis, would prefer forming

complexes with “S-ligands” of GSH and protect proteins from copper-induced damage might explain the inhabitation of GSH for cuproptosis (40). In addition, Zuily and collaborators reported that copper toxicity is related to copper-induced protein aggregation, and treatment with copper (I) under anaerobic conditions leads to severe ROS-independent protein aggregation (41). The knockdown of GLS was associated with the exacerbation of copper toxicity with elesclomol. This evidence highlights the role of GLS in HCC copper-related cell death.

Some limitations existed in our study. First, the construction and validation of the prognostic model were based on retrospective public datasets, thus prospective studies are required to verify the accuracy and utility of our model. Second, some environmental and genetic factors closely related to the occurrence of HCC are inevitably missing. Finally, more *in vivo* and *in vitro* experiments regarding the relationships between cuproptosis-related genes and HCC should be further performed.

Conclusion

In conclusion, a novel CRG, based on cuproptosis-related genes, was constructed using the LASSO Cox regression model. HCC patients with a high CRG scores were revealed to be associated with shorter survival time, lower enrichment in metabolic-related pathways, and high infiltration scores of protumor immune cells. In

our model, among all included CRG genes, GLS was marked as a functional gene in the development of HCC, and might be involved in the cuproptosis process in HCC.

Data availability statement

The datasets presented in this study can be found in online repositories. The names of the repository/repositories and accession number(s) can be found in the article/supplementary material.

Author contributions

(i) Conception and design: BL and JL. (ii) Administrative support: BL and JL. (iii) Experiments implementation: DP and NW. (iv) Data analysis and bioinformatics analysis: GN and YW. (v) Manuscript writing: GN. (vi) Final approval of manuscript: All authors. All authors contributed to the article and approved the submitted version.

Funding

Supported by 1-3-5 project for disciplines of excellence—Clinical Research Incubation Project, West China Hospital, Sichuan

References

- Koren E, Fuchs Y. Modes of regulated cell death in cancer. *Cancer Discovery* (2021) 11(2):245–65. doi: 10.1158/2159-8290.Cd-20-0789
- Jiang X, Stockwell BR, Conrad M. Ferroptosis: Mechanisms, biology and role in disease. *Nat Rev Mol Cell Biol* (2021) 22(4):266–82. doi: 10.1038/s41580-020-00324-8
- Li D, Li Y. The interaction between ferroptosis and lipid metabolism in cancer. *Signal Transduct Target Ther* (2020) 5(1):108. doi: 10.1038/s41392-020-00216-5
- Ye Z, Zhuo Q, Hu Q, Xu X, Mengqi L, Zhang Z, et al. Fbw7-Nra41-Scd1 axis synchronously regulates apoptosis and ferroptosis in pancreatic cancer cells. *Redox Biol* (2021) 38:101807. doi: 10.1016/j.redox.2020.101807
- Tsvetkov P, Coy S, Petrova B, Dreishpoon M, Verma A, Abdusamad M, et al. Copper induces cell death by targeting lipoylated tca cycle proteins. *Science* (2022) 375(6586):1254–61. doi: 10.1126/science.abf0529
- Tang D, Chen X, Kroemer G. Cuproptosis: A copper-triggered modality of mitochondrial cell death. *Cell Res* (2022) 32(5):417–8. doi: 10.1038/s41422-022-00653-7
- Wang Y, Liu T, Li X, Sheng H, Ma X, Hao L. Ferroptosis-inducing nanomedicine for cancer therapy. *Front Pharmacol* (2021) 12:735965. doi: 10.3389/fphar.2021.735965
- Davis CI, Gu X, Kiefer RM, Ralle M, Gade TP, Brady DC. Altered copper homeostasis underlies sensitivity of hepatocellular carcinoma to copper chelation. *Metalomics* (2020) 12(12):1995–2008. doi: 10.1039/d0mt00156b
- Jin C, Li Y, Su Y, Guo Z, Wang X, Wang S, et al. Novel copper complex ctb regulates methionine cycle induced tert hypomethylation to promote hcc cells senescence *Via* mitochondrial Slc25a26. *Cell Death Dis* (2020) 11(10):844. doi: 10.1038/s41419-020-03048-x
- Li Y, Wang LH, Zhang HT, Wang YT, Liu S, Zhou WL, et al. Disulfiram combined with copper inhibits metastasis and epithelial-mesenchymal transition in hepatocellular carcinoma through the nf-kb and tgf- β pathways. *J Cell Mol Med* (2018) 22(1):439–51. doi: 10.1111/jcmm.13334
- Yang M, Wu X, Hu J, Wang Y, Wang Y, Zhang L, et al. Commd10 inhibits Hif1 α /Cp loop to enhance ferroptosis and radiosensitivity by disrupting Cu-fe balance in hepatocellular carcinoma. *J Hepatol* (2022) 76(5):1138–50. doi: 10.1016/j.jhep.2022.01.009
- Pfeiffenberger J, Mogler C, Gotthardt DN, Schulze-Bergkamen H, Litwin T, Reuner U, et al. Hepatobiliary malignancies in Wilson disease. *Liver Int* (2015) 35(5):1615–22. doi: 10.1111/liv.12727
- McEligot AJ, Poynor V, Sharma R, Panagadan A. Logistic lasso regression for dietary intakes and breast cancer. *Nutrients* (2020) 12(9):2652. doi: 10.3390/nu12092652

University (20HXFH021), National Natural Science Foundation of China (Grant No. 82002578).

Conflict of interest

The authors declare that the research was conducted in the absence of any commercial or financial relationships that could be construed as a potential conflict of interest.

Publisher's note

All claims expressed in this article are solely those of the authors and do not necessarily represent those of their affiliated organizations, or those of the publisher, the editors and the reviewers. Any product that may be evaluated in this article, or claim that may be made by its manufacturer, is not guaranteed or endorsed by the publisher.

Supplementary material

The Supplementary Material for this article can be found online at: <https://www.frontiersin.org/articles/10.3389/fonc.2023.1096351/full#supplementary-material>

- Zhang X, Yuan K, Wang H, Gong P, Jiang T, Xie Y, et al. Nomogram to predict mortality of endovascular thrombectomy for ischemic stroke despite successful recanalization. *J Am Heart Assoc* (2020) 9(3):e014899. doi: 10.1161/jaha.119.014899
- Li Z, Zhang H. Reprogramming of glucose, fatty acid and amino acid metabolism for cancer progression. *Cell Mol Life Sci* (2016) 73(2):377–92. doi: 10.1007/s00018-015-2070-4
- Wang Y, Yen FS, Zhu XG, Timson RC, Weber R, Xing C, et al. Slc25a39 is necessary for mitochondrial glutathione import in mammalian cells. *Nature* (2021) 599(7883):136–40. doi: 10.1038/s41586-021-04025-w
- Siddiqui A, Ceppi P. A non-proliferative role of pyrimidine metabolism in cancer. *Mol Metab* (2020) 35:100962. doi: 10.1016/j.molmet.2020.02.005
- Ringelhan M, Pfister D, O'Connor T, Pikarsky E, Heikenwalder M. The immunology of hepatocellular carcinoma. *Nat Immunol* (2018) 19(3):222–32. doi: 10.1038/s41590-018-0044-z
- Tang W, Chen Z, Zhang W, Cheng Y, Zhang B, Wu F, et al. The mechanisms of sorafenib resistance in hepatocellular carcinoma: Theoretical basis and therapeutic aspects. *Signal Transduct Target Ther* (2020) 5(1):87. doi: 10.1038/s41392-020-0187-x
- Tsurusaki M, Murakami T. Surgical and locoregional therapy of hcc: Tace. *Liver Cancer* (2015) 4(3):165–75. doi: 10.1159/000367739
- Solomon EI, Sundaram UM, Machonkin TE. Multicopper oxidases and oxygenases. *Chem Rev* (1996) 96(7):2563–606. doi: 10.1021/cr950046o
- Que EL, Domaille DW, Chang CJ. Metals in neurobiology: Probing their chemistry and biology with molecular imaging. *Chem Rev* (2008) 108(5):1517–49. doi: 10.1021/cr078203u
- Chang CJ. Searching for harmony in transition-metal signaling. *Nat Chem Biol* (2015) 11(10):744–7. doi: 10.1038/nchembio.1913
- Ge EJ, Bush AI, Casini A, Cobine PA, Cross JR, DeNicola GM, et al. Connecting copper and cancer: From transition metal signalling to metalloplasia. *Nat Rev Cancer* (2022) 22(2):102–13. doi: 10.1038/s41568-021-00417-2
- Ren X, Li Y, Zhou Y, Hu W, Yang C, Jing Q, et al. Overcoming the compensatory elevation of Nrf2 renders hepatocellular carcinoma cells more vulnerable to Disulfiram/Copper-induced ferroptosis. *Redox Biol* (2021) 46:102122. doi: 10.1016/j.redox.2021.102122
- Wachsmann J, Peng F. Molecular imaging and therapy targeting copper metabolism in hepatocellular carcinoma. *World J Gastroenterol* (2016) 22(1):221–31. doi: 10.3748/wjg.v22.i1.221

27. Aggarwal A, Bhatt M. Advances in treatment of Wilson disease. *Tremor Other Hyperkinet Mov (N Y)* (2018) 8:525. doi: 10.7916/d841881d
28. Fang AP, Chen PY, Wang XY, Liu ZY, Zhang DM, Luo Y, et al. Serum copper and zinc levels at diagnosis and hepatocellular carcinoma survival in the guangdong liver cancer cohort. *Int J Cancer* (2019) 144(11):2823–32. doi: 10.1002/ijc.31991
29. Tamai Y, Iwasa M, Eguchi A, Shigefuku R, Sugimoto K, Hasegawa H, et al. Serum copper, zinc and metallothionein serve as potential biomarkers for hepatocellular carcinoma. *PLoS One* (2020) 15(8):e0237370. doi: 10.1371/journal.pone.0237370
30. Mukha A, Kahya U, Linge A, Chen O, Löck S, Lukiyanchuk V, et al. Gls-driven glutamine catabolism contributes to prostate cancer radiosensitivity by regulating the redox state, stemness and Atg5-mediated autophagy. *Theranostics* (2021) 11(16):7844–68. doi: 10.7150/thno.58655
31. Li B, Cao Y, Meng G, Qian L, Xu T, Yan C, et al. Targeting glutaminase 1 attenuates stemness properties in hepatocellular carcinoma by increasing reactive oxygen species and suppressing Wnt/Beta-catenin pathway. *EBioMedicine* (2019) 39:239–54. doi: 10.1016/j.ebiom.2018.11.063
32. Foulkes WD, Flanders TY, Pollock PM, Hayward NK. The Cdkn2a (P16) gene and human cancer. *Mol Med* (1997) 3(1):5–20.
33. Luo JP, Wang J, Huang JH. Cdkn2a is a prognostic biomarker and correlated with immune infiltrates in hepatocellular carcinoma. *Biosci Rep* (2021) 41(10):BSR20211103. doi: 10.1042/bsr20211103
34. Saudino G, Ciofi-Baffoni S, Banci L. Protein-interaction affinity gradient drives [4fe-4s] cluster insertion in human lipoyl synthase. *J Am Chem Soc* (2022) 144(13):5713–7. doi: 10.1021/jacs.1c13626
35. Burr SP, Costa AS, Grice GL, Timms RT, Lobb IT, Freisinger P, et al. Mitochondrial protein lipoylation and the 2-oxoglutarate dehydrogenase complex controls Hif1 α stability in aerobic conditions. *Cell Metab* (2016) 24(5):740–52. doi: 10.1016/j.cmet.2016.09.015
36. Miao X, Leng X, Zhang Q. The current state of nanoparticle-induced macrophage polarization and reprogramming research. *Int J Mol Sci* (2017) 18(2):336. doi: 10.3390/ijms18020336
37. Italiani P, Boraschi D. From monocytes to M1/M2 macrophages: Phenotypical vs. *Funct Differentiation. Front Immunol* (2014) 5:514. doi: 10.3389/fimmu.2014.00514
38. Wang D, Meng G, Zheng M, Zhang Y, Chen A, Wu J, et al. The glutaminase-1 inhibitor 968 enhances dihydroartemisinin-mediated antitumor efficacy in hepatocellular carcinoma cells. *PLoS One* (2016) 11(11):e0166423. doi: 10.1371/journal.pone.0166423
39. Chung CY, Posimo JM, Lee S, Tsang T, Davis JM, Brady DC, et al. Activity-based ratiometric fret probe reveals oncogene-driven changes in labile copper pools induced by altered glutathione metabolism. *Proc Natl Acad Sci U.S.A.* (2019) 116(37):18285–94. doi: 10.1073/pnas.1904610116
40. Kardos J, Héja L, Simon Á, Jablonkai I, Kovács R, Jemnitz K. Copper signalling: Causes and consequences. *Cell Commun Signal* (2018) 16(1):71. doi: 10.1186/s12964-018-0277-3
41. Zuily L, Lahrach N, Fassler R, Genest O, Faller P, Sénèque O, et al. Copper induces protein aggregation, a toxic process compensated by molecular chaperones. *mBio* (2022) 13(2):e0325121. doi: 10.1128/mbio.03251-21